

FIRST OBSERVATION IN THE SOUTH OF TITAN'S FAR-INFRARED 220 cm⁻¹ CLOUD

DONALD E. JENNINGS¹, C. M. ANDERSON¹, R. E. SAMUELSON^{1,2}, F. M. FLASAR¹, C. A. NIXON¹, G. L. BJORAKER¹, P. N. ROMANI¹,
R. K. ACHTERBERG^{1,2}, V. COTTINI¹, B. E. HESMAN^{1,2}, V. G. KUNDE^{1,2}, R. C. CARLSON^{1,3}, R. DE KOK⁴, A. COUSTENIS⁵,
S. VINATIER⁵, G. BAMPASIDIS^{5,6}, N. A. TEANBY⁷, AND S. B. CALCUTT⁸

¹ Goddard Space Flight Center, Greenbelt, MD 20771, USA; donald.e.jennings@nasa.gov

² Department of Astronomy, University of Maryland, College Park, MD 20742, USA

³ IACS, The Catholic University of America, Washington, DC 20064, USA

⁴ SRON Netherlands Institute for Space Research, Sorbonnelaan 2, 3584 CA Utrecht, The Netherlands

⁵ LESIA, Observatoire de Paris-Meudon, 92195 Meudon Cedex, France

⁶ Faculty of Physics, National and Kapodistrian University of Athens, Panepistimioupolis, GR 15783 Zographos, Athens, Greece

⁷ School of Earth Sciences, University of Bristol, Bristol BS8 1RJ, UK

⁸ Department of Physics, University of Oxford, Parks Road, Oxford OX1 3PU, UK

Received 2012 October 23; accepted 2012 November 8; published 2012 November 26

ABSTRACT

An emission feature at 220 cm⁻¹ which has been attributed to a cloud of condensed material in Titan's winter stratosphere has been seen for the first time in the south. This feature had previously been found only at high northern latitudes during northern winter and spring. The material emitting at 220 cm⁻¹, as yet unidentified, may be volatiles associated with nitrile gases that accumulate in the absence of ultraviolet sunlight. Not detected as recently as 2012 February, the 220 cm⁻¹ feature clearly appeared at the south pole in *Cassini* spectra recorded on 2012 July 24, indicating a rapid onset of the emission. This is the first indication of the winter buildup of condensation in the southern stratosphere that has been expected as the south pole moves deeper into shadow. In the north the 220 cm⁻¹ feature continued to decrease in intensity with a half-life of 3 years.

Key words: molecular processes – planets and satellites: atmospheres – planets and satellites: composition – planets and satellites: individual (Titan) – radiation mechanisms: thermal

Online-only material: color figures

1. INTRODUCTION

An overarching goal of the *Cassini* Solstice Mission is to study the seasonal evolution of Titan's atmosphere. As Titan has emerged from northern winter, *Cassini* has witnessed shifts in photochemical hazes (West et al. 2011; Jennings et al. 2012), temperature structure (Achterberg et al. 2011) and composition (Teanby et al. 2008, 2010, 2012; Vinatier et al. 2012a; Bampasidis et al. 2012). Seasonal changes are most extreme at the poles, where darkness is uninterrupted during deep winter. Lower temperatures in the winter shadow, combined with material migration toward the winter pole, cause a buildup of organic vapors and condensates in the stratosphere. In both *Voyager* and *Cassini* visible images the haze has a north–south asymmetry and a conspicuous haze “hood” covering latitudes beyond about 55°N (Sromovsky et al. 1981; Porco et al. 2005). Cloud and haze concentrations in the north are also seen in near-infrared images (Griffith et al. 2006) and far-infrared spectra (Cottini et al. 2012; Anderson & Samuelson 2011; Vinatier et al. 2010a, 2012b; de Kok et al. 2007; Samuelson et al. 2007; Teanby et al. 2012). Recent *Cassini* images of Titan's south pole show the formation of a haze hood and polar vortex, signs that the south is reacting to the coming of winter and may replicate the seasonal character of the north (West et al. 2012).

We previously reported a four-fold seasonal decrease in intensity of the unidentified feature at 220 cm⁻¹ in the spectrum of Titan's northern stratosphere, observed by *Cassini* over the period 2004–2012 (Jennings et al. 2012). We now report the first appearance of this feature in the south. Seen first by the Infrared Interferometer Spectrometer (IRIS) on *Voyager 1* (Kunde et al. 1981; Coustenis et al. 1999), this emission feature has been observed extensively by the Composite Infrared Spectrometer

(CIRS) on *Cassini* (Flasar et al. 2004; de Kok et al. 2007, 2008; Samuelson et al. 2007; Anderson et al. 2012). The spectral feature, which never appears at mid-latitudes, is bell-shaped and approximately 30 cm⁻¹ wide (FWHM). Most likely due to a cloud of condensed material, in the north the emission arises from 80 to 150 km in altitude and peaks sharply in opacity near 140 km (de Kok et al. 2007, 2008; Anderson et al. 2012). Although simple molecules have been largely ruled out for the source of the condensate (Dello Russo & Khanna 1996; Coustenis et al. 1999; Samuelson et al. 2007), indirect evidence points to volatiles of a nitrile origin (Coustenis et al. 1999; de Kok et al. 2008; Jennings et al. 2012).

2. OBSERVATIONS

South pole limb spectra of Titan were recorded by CIRS during 21 *Cassini* flybys between 2005 April and 2012 July. The spectra covered 10–600 cm⁻¹ with a resolution of 15 cm⁻¹. For each flyby we averaged limb spectra in the latitude range 70–90°S (here the term “limb” means the atmosphere just beyond Titan's solid body diameter). Among the flybys the number of averaged spectra varied between 1 and 203. We selected limb data for which the CIRS field of view (FOV) was centered at a tangent point located between 40 and 160 km above the surface. This range was chosen to bracket the 80–150 km altitude where the 220 cm⁻¹ emission has been found to arise in the north (Anderson et al. 2012; de Kok et al. 2007). The distance of the spacecraft to the limb varied among the flybys between 12,000 and 185,000 km. These data selection criteria matched those used by Jennings et al. (2012) in their study of the 220 cm⁻¹ feature in the north polar region. Examples of the spectra from three recent flybys are shown in Figure 1. The 220 cm⁻¹ feature was not present in the spectrum from

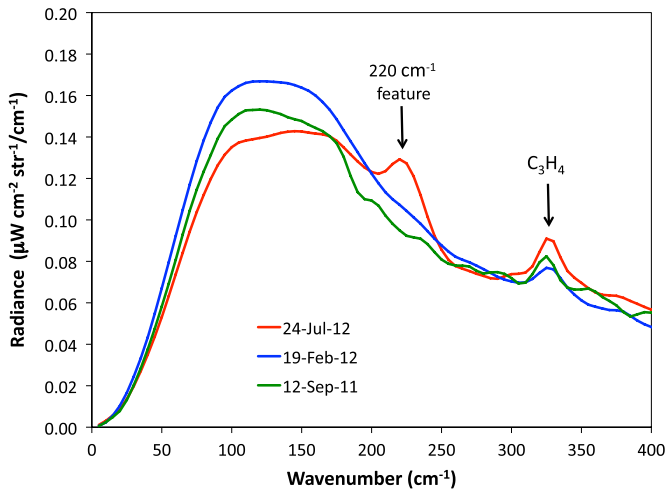


Figure 1. Three spectra observed near Titan’s south pole showing the emergence of the 220 cm^{-1} feature in 2012 July. The observations were at the limb, but the FOV’s overlapped onto the disk. Latitudes and spacecraft ranges were: for 2011 September 12, 73°S and $25,000\text{ km}$; for 2012 February 19, 80°S and $56,000\text{ km}$; and for 2012 July 24, 74°S and $50,000\text{ km}$.

(A color version of this figure is available in the online journal.)

2011 September 12 or from 2012 February 19, 2012, but it then appeared prominently in the limb spectrum on 2012 July 24 for the first time in the mission.

3. DATA ANALYSIS

The observing geometries (spacecraft distance, tangent height, emission angle) varied considerably among the flybys and among individual spectra of each flyby. Furthermore, the field of view ranged from 42 to 648 km among the observations. Thus, the field of view usually subtended not only the limb but also part of the disk and deep space. To avoid difficulties in modeling the spectra, we derived the relative intensity of the 220 cm^{-1} emission using the method adopted by Jennings et al. (2012). In each flyby spectrum we measured the peak radiances, above their local continua, of the 220 cm^{-1} feature and the C_3H_4 band at 325 cm^{-1} (see Figure 1). These two peak radiances were then ratioed: $220\text{ cm}^{-1}/325\text{ cm}^{-1}$. Figure 2 shows the ratios for the 21 flybys that viewed the south pole. The C_3H_4 band in the far-IR serves as a reliable intensity reference because (1) it has been relatively constant over the mission, (2) it is formed at stratospheric altitudes similar to the 220 cm^{-1} emission, and (3) both emission features are optically thin. We calculated the peak radiances of the features by subtracting the average of the continua at the wings of each feature from the total radiance at the center of the feature. The continuum in the vicinity of 220 cm^{-1} tended to be convex, so that in the absence of emission from the 220 cm^{-1} feature the pure continuum at the 220 cm^{-1} was below the average of the continua at the wings. This gave a negative value for the 220 cm^{-1} peak radiance and also a negative value for the $220\text{ cm}^{-1}/325\text{ cm}^{-1}$ ratio. To find the correction for this zero bias, we averaged spectra outside the polar region where the 220 cm^{-1} feature was absent. We determined that zero radiance from the 220 cm^{-1} feature gave a ratio of -0.3 and we applied this correction to all ratios before plotting them in Figure 2.

Two gas species, C_4H_2 and C_2N_2 , have rotation–vibration bands within the width of the 220 cm^{-1} feature. To determine how much of the observed emission is from these gases we calculated a synthetic spectrum without the 220 cm^{-1} feature.

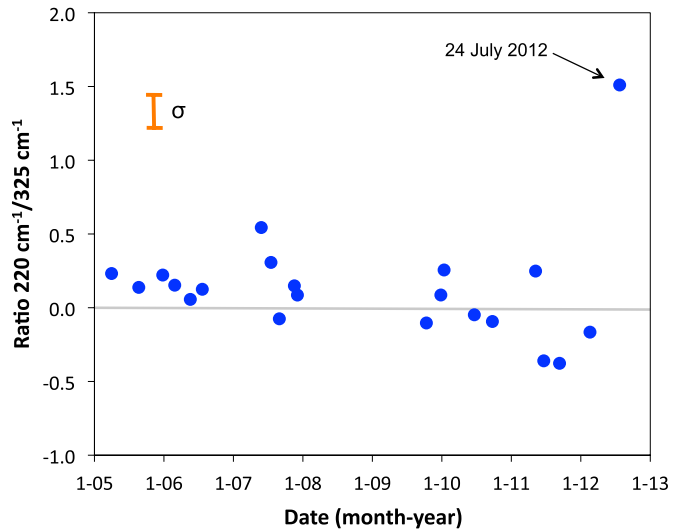


Figure 2. Intensities of the emission feature at 220 cm^{-1} from Titan’s south pole limb measured as the ratios of the 220 cm^{-1} peak to the peak of the C_3H_4 band at 325 cm^{-1} . The emission feature was undetectable from 2005 April to 2012 February, but then appeared in the latest observation on 2012 July 24. Each data point represents an average of spectra from 70°N to 90°N for the Titan flyby date plotted. The 1σ error bar shown is the standard deviation from the average of all of the data points except 2012 July.

(A color version of this figure is available in the online journal.)

Our modeling showed that the shape of the feature would be significantly different from the observed shape if the emission was purely due to C_4H_2 and C_2N_2 . From the model we estimate that these gases contribute no more than 0.2 to each of the $220\text{ cm}^{-1}/325\text{ cm}^{-1}$ ratios plotted in Figure 2 (i.e., the ratios include the gases). The ratios reported by Jennings et al. (2012) for the north also include emission from C_4H_2 and C_2N_2 gas. No correction was made for the gas contribution.

4. RESULTS AND DISCUSSION

As Figure 2 shows, the 220 cm^{-1} intensity was not detected at the south pole beginning with the first CIRS observation in 2005 April and up to as recently as 2012 February. Then in 2012 July, three years after equinox, the intensity suddenly became visible and the $220\text{ cm}^{-1}/325\text{ cm}^{-1}$ ratio jumped to 1.5. Meanwhile, in the north this feature, which had been strong at the beginning of the mission, had greatly decreased in intensity (Jennings et al. 2012) and in 2012 July was comparable to its counterpart in the south. The increase of the emission in the south was much faster than the decrease in the north. In the north the 220 cm^{-1} intensity had been decreasing by about a factor of two every three years, whereas in the south it increased by a factor of at least four within six months. In Figure 3, we place the 220 cm^{-1} observations from both north and south on a common seasonal scale. We use seasonal phase as a coordinate because it is independent of northern or southern hemisphere (the more conventional solar longitude gives the season only when the hemisphere is specified). The intensities during winter and spring are represented by the northern data from Jennings et al. (2012), plus an additional northern data point for 2012 July 24. The summer and autumn intensities are represented by the southern data from Figure 2. In Figure 3 we have converted the $220\text{ cm}^{-1}/325\text{ cm}^{-1}$ ratios to radiances for the 220 cm^{-1} feature (measured with respect to the continuum). We did this by scaling to the highest limb radiance in our dataset; $0.31\text{ }\mu\text{W cm}^{-2}\text{ str}^{-1}/\text{cm}^{-1}$ was measured at close range on

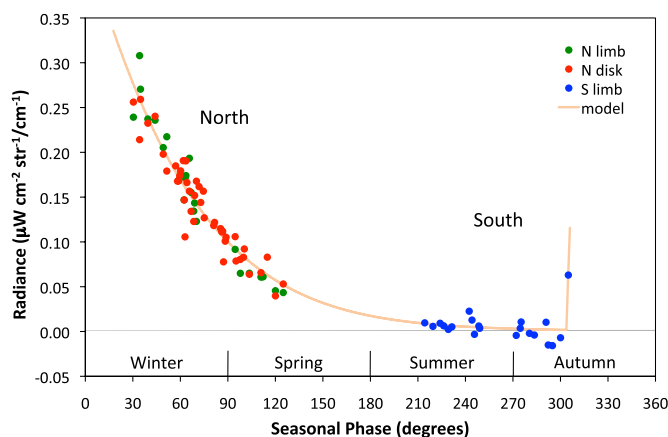


Figure 3. North and south polar radiances of the 220 cm^{-1} feature plotted on the same seasonal scale. Data from Titan’s north represents winter–spring behavior and the data from the south represents summer–autumn behavior. The northern values were adapted from Jennings et al. (2012), with the addition of a data point in the north from 2012 July 24. The southern values are from Figure 2 in this paper. The seasonal phase scale begins at winter solstice and each 30° increment equals one Titan month. The model is described in the text.

(A color version of this figure is available in the online journal.)

2005 March 31. Although we do not believe that the seasonal behavior in the north and south are exactly the same, we assume that they are similar enough to give us an approximate picture of the seasonal cycle of the 220 cm^{-1} ice cloud. As can be seen in the figure, the decrease of emission from the northern cloud in late winter and early spring is approximately exponential with a half-life of 3 years or 1.3 Titan-months. The intensity approaches zero in late summer and early autumn, as shown by the southern data. Two Titan months before winter solstice the emission abruptly reappears, presumably as the cloud begins a new cycle.

The advent of the 220 cm^{-1} feature in 2012 coincides with the rapid development of a high–altitude haze hood and vortex at the south pole seen by the Imaging Science Subsystem (ISS) and Visible and Infrared Mapping Spectrometer (VIMS) on *Cassini* (West et al. 2012; see also *Cassini* images PIA14913, PIA15609, PIA14919). A change in the haze structure at the pole was first noticed in 2011 September and first signs of a haze hood were apparent in 2012 March. Images taken on June 27, 2012 showed that a vortex a few degrees in extent had formed at the south pole. With the approach of winter the global atmospheric circulation may have switched from north to south. As the seasons progress, the southern vortex and haze hood are expected to mirror the by now familiar winter structures at the north pole. Formation of winter structures at the south pole signals the accumulation of material at high altitude, some of which migrates downward and become available for cloud formation. Molecules that are created in sunlight above 600 km are protected by the polar shadow from ultraviolet destruction during their decent to the stratospheric cloud height at $\sim 150\text{ km}$ (Yung 1987).

The near-simultaneous appearances of the 220 cm^{-1} feature and the polar haze hood might mean that we are detecting emission from material in the new hood itself. West et al. (2012) have suggested that the inhomogeneous appearance of the haze in the ISS images may be due to condensation in the vortex, and this could be the same condensate that we are seeing at 220 cm^{-1} . Although the opacity of the 220 cm^{-1} ice cloud in mid-northern winter has been shown to have a broad range in altitude from 80 to 150 km with a peak at 140 km (de Kok et al. 2007), a different distribution during the early

formation in autumn is not precluded by our observations. West et al. (2012) determined a height of 320 km for the new polar haze layer. Although the CIRS field of view on 2012 July 24 was centered at tangent heights only as high as 250 km, the pole was tilted 16 degrees toward the spacecraft at the time of the observations and the haze layer was therefore at least partially within the CIRS field of view over a wide range of tangent altitudes. CIRS’ 175 km diameter field of view in these observations makes it impossible to determine the precise height of the emitting substance, but the possibility remains that we are seeing emission from the polar hood.

Stratospheric cloud formation begins when the combination of temperature and molecular density of a gas surpasses its saturation limit and condensation sets in. In Titan’s stratosphere condensation was almost certainly initiated by the decline in temperatures in the deepening polar shadow. At high southern latitudes Teanby et al. (2012) have found that the temperature near 200 km altitude dropped from 170 K to 150 K between early 2010 and late 2011. This is akin to what has been seen at high northern latitudes during winter, where stratospheric temperatures were depressed 20–40 K below typical equatorial temperatures (Teanby et al. 2007; Coustenis et al. 2010; Achterberg et al. 2008, 2011; Schinder et al. 2012). We propose that in 2012 atmospheric gases began to condense in response to the falling temperatures. The swift onset of cloud formation might be a sign that the gas reached supersaturation, initiating spontaneous nucleation and very rapid condensation. In any case, condensation can be expected to continue until the temperature stabilizes, at which point the cloud growth will slow or halt. The supply of gases from the upper atmosphere will eventually weaken and the cloud will gradually be depleted through precipitation. The empirical model shown in Figure 3 attempts to capture this behavior. We assume that the cloud radiance is proportional to its density, which in turn is governed by condensation and precipitation. In the model, the condensation rate increases instantaneously at a seasonal phase of 305° , before winter solstice. We assume that condensation ends after a short period. Following winter solstice the cloud material precipitates out and the cloud density decreases exponentially. We adjusted the model amplitude and decay constant to match the observed radiances and from this we derived a half-life for the cloud density of 1.3 Titan-months. This empirical model is only one possible description of the seasonal behavior of the gas; for example, a longer period of condensation is compatible with the data provided that the decrease in condensation is exponential after winter solstice and that it ceases by summer. Although this model may be somewhat simplistic, it indicates that the observed radiances in the north and south are consistent with a cloud that forms very quickly and then disappears more slowly through precipitation. The data and model further suggest that the processes that create and destroy the cloud are not symmetric about the winter solstice.

Do our results add any information about the composition of the 220 cm^{-1} cloud? Nitriles have been proposed as candidates for the cloud material (Coustenis et al. 1999; Dello Russo & Khanna 1996; Khanna 2005; de Kok 2008; Jennings et al. 2012) and our observations lend support to that possibility. Judging from CIRS data, nitriles were building up at the south pole about a year before the 220 cm^{-1} feature was first seen. Our observations in the south (Nixon et al. 2012) show that HC_3N , which may serve as a tracer of complex nitriles, was present in 2011 November spectra but not in 2011 January spectra, implying that the nitrile increase started in mid-2011.

Stratospheric cooling by 20–40 K in the polar night (Teanyby et al. 2007, 2012; Coustenis et al. 2010; Achterberg et al. 2008, 2011; Schinder et al. 2012) would raise the nitrile condensation altitude from ~ 90 km (Lara et al. 1996) to ~ 150 km, near the top of the 220 cm^{-1} cloud. Indeed, Anderson et al. (2010) found condensed HC_3N at 150 and 165 km during northern winter at latitudes of 65N and 70N. Furthermore, in northern winter HC_3N exhibited a more pronounced increase than any other molecule toward high northern latitudes where the 220 cm^{-1} cloud resides (Teanyby et al. 2008; Coustenis et al. 2010; Vinatier et al. 2010b). Finally, during winter and spring in the north HC_3N underwent an overall decrease in abundance, following the same trend as the 220 cm^{-1} cloud (Vinatier et al. 2012a; Jennings et al. 2012). Taken together, the evidence points to a close relationship between nitrile gases and the 220 cm^{-1} cloud. We caution, however, that if the south pole emission arises from the haze layer identified at 320 km by West et al. (2012), the conditions at that altitude would make it more difficult to explain the presence of condensed nitriles.

CIRS will continue to observe changes in the 220 cm^{-1} emission feature in the north and south until the end of the *Cassini* mission in 2017. We will track not only the feature itself, but, indirectly, the gaseous source of the condensibles and the precipitation from the stratosphere to the surface. By observing both hemispheres for almost one-half of a Titan year *Cassini* is giving us a nearly complete picture of Titan's yearly cycle.

We acknowledge support from NASA's *Cassini* mission, *Cassini* Data Analysis Program and Planetary Astronomy Program. V.C. was supported by the NASA Postdoctoral Program. N.A.T. was supported by the UK STFC and the Leverhulme Trust. We thank Robert West for pointing out that we might be seeing emission from the south polar hood.

REFERENCES

- Achterberg, R. K., Conrath, B. J., Gierasch, P. J., Flasar, F. M., & Nixon, C. A. 2008, *Icarus*, 194, 263
- Achterberg, R. K., Gierasch, P. J., Conrath, B. J., Flasar, F. M., & Nixon, C. A. 2011, *Icarus*, 211, 686
- Anderson, C. M., & Samuelson, R. E. 2011, *Icarus*, 212, 762
- Anderson, C. M., Samuelson, R. E., & Achterberg, R. K. 2012, Titan Through Time 2; Unlocking Titan's Past, Present and Future (Greenbelt, MD: NASA Goddard Space Flight Center)
- Anderson, C. M., Samuelson, R. E., Bjoraker, G. L., & Achterberg, R. K. 2010, *Icarus*, 207, 914
- Bampasidis, G., Coustenis, A., Achterberg, R. K., et al. 2012, *ApJ*, 760, 144
- Cottini, V., Nixon, C. A., Jennings, D. E., et al. 2012, *Planet. Space Sci.*, 60, 62
- Coustenis, A., Jennings, D. E., Nixon, C. A., et al. 2010, *Icarus*, 207, 461
- Coustenis, A., Schmitt, B., Khanna, B., & Trotta, F. 1999, *Planet. Space Sci.*, 47, 1305
- de Kok, R., Irwin, P. G. J., Teanyby, N. A., et al. 2007, *Icarus*, 191, 223
- de Kok, R., Irwin, P. G. J., & Teanyby, N. A. 2008, *Icarus*, 197, 572
- Dello Russo, N., & Khanna, R. K. 1996, *Icarus*, 123, 366
- Griffith, C. A., Penteado, P., Rannou, P., et al. 2006, *Science*, 313, 1620
- Flasar, F. M., Kunde, V. G., Abbas, M. M., et al. 2004, *Space Sci. Rev.*, 115, 169
- Jennings, D. E., Anderson, C. M., Samuelson, R. E., et al. 2012, *ApJ*, 754, L3
- Khanna, R. K. 2005, *Icarus*, 177, 116
- Kunde, V. G., Aikin, A. C., Hanel, R. A., et al. 1981, *Nature*, 292, 686
- Lara, L. M., Lellouch, E., Lopez-Moreno, J. J., & Rodrigo, R. 1996, *J. Geophys. Res.*, 101, 23, 261
- Nixon, C. A., Bjoraker, G. L., Achterberg, R. K., et al. 2012, *BAAS*, 44, 312.19
- Porco, C. C., Baker, E., Barbara, J., et al. 2005, *Nature*, 434, 159
- Samuelson, R. E., Smith, M. D., Achterberg, R. K., & Pearl, J. C. 2007, *Icarus*, 189, 63
- Schinder, P. J., Flasar, F. M., Marouf, E. A., et al. 2012, *Icarus*, 221, 1020
- Sromovsky, L. A., Suomi, V. E., & Pollack, J. B. 1981, *Nature*, 292, 698
- Teanyby, N. A., Irwin, P. G. J., de Kok, R., & Nixon, C. A. 2010, *ApJ*, 724, L84
- Teanyby, N. A., Irwin, P. G. J., de Kok, R., et al. 2007, *Icarus*, 186, 364
- Teanyby, N. A., Irwin, P. G. J., de Kok, R., et al. 2008, *Icarus*, 193, 595
- Teanyby, N. A., Irwin, P. G. J., Nixon, C. A., et al. 2012, *Nature*, in press
- Vinatier, S., Bézard, B., Coustenis, A., et al. 2012a, Paper EPSC2012-569 presented at The European Planetary Science Congress, September 23–28, Madrid, Spain
- Vinatier, S., Bézard, B., de Kok, R., et al. 2010a, *Icarus*, 210, 852
- Vinatier, S., Bézard, B., Nixon, C. A., et al. 2010b, *Icarus*, 205, 559
- Vinatier, S., Rannou, P., Anderson, C. M., Bézard, B., de Kok, R., & Samuelson, R. E. 2012b, *Icarus*, 219, 5
- West, R. A., Balloch, J., Dumont, P., et al. 2011, *Geophys. Res. Lett.*, 38, L06204
- West, R. A., Del Genio, A., & Perry, J. 2012, *BAAS*, 44, 300.04
- Yung, Y. L. 1987, *Icarus*, 72, 468